

DOI: 10.1002/cbic.201600655



Studies of the Binding of Modest Modulators of the Human Enzyme, Sirtuin 6, by STD NMR

Beatriz E. Bolívar and John T. Welch*[a]

Pyrazinamide (PZA), an essential constituent of short-course tuberculosis chemotherapy, binds weakly but selectively to Sirtuin 6 (SIRT6). Despite the structural similarities between nicotinamide (NAM), PZA, and pyrazinoic acid (POA), these inhibitors modulate SIRT6 by different mechanisms and through different binding sites, as suggested by saturation transfer difference (STD) NMR. Available experimental evidence, such as that derived from crystal structures and kinetic experiments, has been of only limited utility in elucidation of the mechanistic details of sirtuin inhibition by NAM or other inhibitors. For instance, crystallographic structural analysis of sirtuin binding sites does not help us understand important differences in binding affinities among sirtuins or capture details of such dynamic process.

Hence, STD NMR was utilized throughout this study. Our results not only agreed with the binding kinetics experiments but also gave a qualitative insight into the binding process. The data presented herein suggested some details about the geometry of the binding epitopes of the ligands in solution with the apo- and holoenzyme. Recognition that SIRT6 is affected selectively by PZA, an established clinical agent, suggests that the rational development of more potent and selective NAM surrogates might be possible. These derivatives might be accessible by employing the malleability of this scaffold to assist in the identification by STD NMR of the motifs that interact with the apo- and holoenzymes in solution.

Introduction

Mammalian sirtuins (SIRTs), class III histone deacetylases (HDAC), are homologues of the yeast silent information regulator 2 (Sir2). SIRTs possess unique NAD⁺-dependent enzymatic activities and share no sequence homology with the classical HDACs.^[1] SIRTs contain a highly conserved catalytic domain with many of the specific requirements for NAD⁺ binding, such as the G-X-G motif, important for recognition of the phosphate group, and the presence of charged residues that allow binding of the two ribose groups. The adenine base of NAD⁺ binds the C-terminal half of this domain^[2] at a partially hydrophobic pocket, called the A-site. The NAM ribose moiety, whose conformation has been shown to vary among structures, binds to the B-site, whereas the pyridine carboxamide moiety binds to the C-site^[3] (Figure 1 A).

SIRTs, implicated in caloric restriction, aging, and inflammation, [4] regulate many cellular processes such as transcriptional repression, recombination, cell cycle division, microtubule organization, insulin secretion, and cell death mechanisms. [5] SIRTs are further phylogenetically classified into four subclasses based on homology of their 250 amino acid core domain. NAD+-dependent deacylation of a protein is the most common reaction catalyzed by sirtuins, in which one molar equivalent of NAD+ is consumed per lysine acyl group removed, pro-

ducing nicotinamide (NAM) and 2'-O-acetyl-ADP-ribose in the process. $^{\rm [6]}$

SIRT6, a class IV sirtuin, is a nuclear protein that is a closely related functional orthologue of the single yeast sirtuin (Sir2) gene. [7] SIRT6 was initially described as a self mono-ADP-ribosyltransferase^[8] but was subsequently recognized as an NAD⁺dependent deacetylase, with a high degree of intrinsic substrate selectivity for Lys9 and Lys56 of histone 3, H3K9Ac, and H3K56Ac. [9] The interaction between Lys9 and Lys56 is associated with the role of SIRT6 in DNA damage response under oxidative stress and in telomere maintenance. [9b,10] SIRT6 also catalyzes the hydrolysis of fatty acyl lysine modifications efficiently. SIRT6 regulates the fatty acylation level on Lys19 and Lys20 of TNF α , and hence controls the secretion of TNF α . Interestingly, Denu and collaborators found that free fatty acids (FFAs) activate deacetylation. Conversely, FFAs appear to inhibit de-fatty acylation, leading to their hypothesis that FFAs possibly bind to the same acyl group binding pocket and induce closure of the Rossman fold domain and the zinc-binding domain, a conformational change that could induce canonical active site conformation and thus increase the deacetylase activity.[11]

SIRT6 is an interesting target for the development of agents against pro-inflammatory autoimmune, inflammatory, and other degenerative diseases. [12] SIRT6 regulates the expression of a large number of stress-responsive and metabolism-related genes, as well as the activity of several transcription factors implicated in the immune response. SIRT6-mediated deacetylation of His3 is central to maintenance of chromatin integrity in telomeres [96,13] and to regulation of gene expression through recruitment by transcription factors (e.g., NF- κ B, HIF1 α). [9c,12] A

Supporting information and the ORCID identification numbers for the authors of this article can be found under http://dx.doi.org/10.1002/chic.201600655

Wiley Online Library

 [[]a] B. E. Bolívar, Prof. J. T. Welch
 Department of Chemistry, University at Albany
 1400 Washington Avenue, Albany, NY 12205 (USA)
 E-mail: jwelch@albany.edu

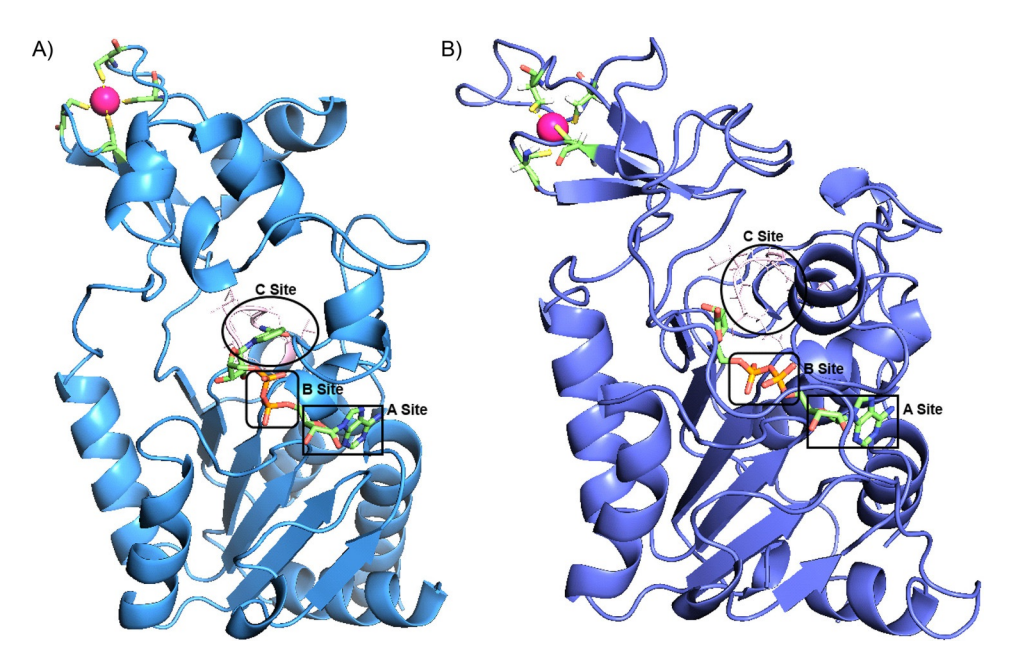


Figure 1. Crystal structure of the complexes Sir2Af2–NAD⁺ and SIRT6–ADPr, highlighting the active site pockets A, B, and C. The Protein Data Bank ID for Sir2Af2 is 1S7G (1 A) and for SIRT6 is 3ZG6 (1 B).

stress-responsive transcription factor, NF- κ B induces expression of target genes involved in aging-related processes, including cell senescence, apoptosis, and inflammation. [9c] SIRT6 binds to the NF- κ B subunit RelA and attenuates NF- κ B signaling by modifying chromatin at NF- κ B target genes. Upon binding, SIRT6 deacetylates His3–Lys9 of the promoters of NF- κ B genes, destabilizing the NF- κ B complex–DNA interaction and repressing expression of NF- κ B-related genes. [9c]

The regulatory role of these enzymes defines the need for detailed studies of the chemical mechanism by which each of the SIRTs is modulated. Despite the high homology among SIRTs, functional differentiation between distinct substrates and activity levels is not sufficient for extrapolation. Although all sirtuins undergo some level of base exchange inhibition by NAM, sirtuins have evolved diverse mechanisms for regulation by NAM that are suited to the particular physiological role of the enzyme, just as different mechanisms have evolved for association with NAD+. Sir2Af2 is only partially inhibited by NAM, whereas the mammalian SIRT1 is completely inhibited by NAM.[14] In our studies, regulation of SIRT6 by NAM prompted the mechanistic characterization of SIRT6 inhibition by NAM and NAM analogues, as well as investigation of the influence of conformational changes on catalysis, substrate specificity, and the inhibitory mechanism.

In our in vitro experiments, we observed that the antituber-culosis drug pyrazinamide (PZA) modestly inhibits the NAD⁺-dependent deacylase enzyme SIRT6. In the 1950s, PZA was the most active synthetic analogue of NAM found in a murine model of tuberculosis (TB).^[15] In spite of poor in vitro activity, PZA is an essential constituent of the current first-line treatment for TB. In combination with isoniazid and rifampin, PZA has been suggested to be active against intracellular mycobacterial organisms thought to be responsible for TB relapse.^[16] Recently, a modulatory role in the host immune response was

www.chembiochem.org

attributed to PZA,^[17] but the detailed mechanism of action of PZA is not yet definitively established. We found that PZA and its active metabolite, POA, appeared to weakly bind SIRT6. However, functionalization of the PZA scaffold resulted in enhanced affinity for the enzyme. In this work, we elaborated on the interactions of NAM, PZA, and POA with host enzyme SIRT6 and utilized those findings to attempt elucidate a better understanding of SIRT6 inhibition.

Results and Discussion

PZA selectively inhibits SIRT6

The activity of PZA and PZA analogue 5-chloro-pyrazinamide (5-Cl-PZA) was assessed against four of the human sirtuins—SIRT1, 2, 3, and 6—in a fluorimetric assay with the labeled peptide Ac-p53 (Ac-Arg-His-Lys-Lys (Ac)-AMC). Of the sirtuins tested, nuclear sirtuins 1 and 6, which are involved in NF- κ B modulation, and hence inflammation, were the only sirtuins that displayed a response to PZA and 5-Cl-PZA. Substitution at the 5-position of the pyrazine ring resulted in increased enzyme affinity, suggesting potential improvements in efficacy, selectivity, and affinity for these sirtuins by rational modification of the pyrazine scaffold.

Subsequently, the IC_{50} values of NAM, PZA, and analogues were determined by using the same fluorescence-based coupled-enzyme assay^[18] with 10.8 μ M SIRT6, 270 μ M Ac-p53 and 1 mM NAD⁺. These assays helped establish relative inhibitor potency with respect to the natural inhibitor, NAM (Table 1). With higher IC_{50} values, both PZA and POA were less effective than NAM. However, methoxy or chloro substitution at the 5-position of the pyrazine ring decreased the IC_{50} value by one order of magnitude. Determination of the nature of the enzyme interactions and the mechanism of inhibition are nec-

5-CI-PZA

Table 1. IC ₅₀ value (270 μм), and NAD	es determined by using SIRTo $^+$ (1 mm).	б (10.8 μм), Ас-р53
Compound	Structure	IC ₅₀ [mм]
NAM	NH ₂	0.1894±0.0735
PZA	NH ₂	0.4169 ± 0.1504
POA	OH	0.9268 ± 0.2495
5-MeO-PZA	N NH_2	0.0404±0.0272

Data shown are an average of at least three replicates with standard deviations.

 0.0332 ± 0.0101

essary to ascertain whether the interactions are specific or non-specific.

PZA and POA modestly modulate SIRT6

To further investigate the nature of PZA and POA interactions with SIRT6, steady-state kinetic analyses of the influence of the concentration of acetylated substrate, Ac-p53, and then of concentrated cofactor NAD+ were completed. Firstly, the inhibitory mechanism relative to substrate Ac-p53 was established. Dixon analysis was utilized, in this case, as it requires fewer substrate concentration data points. Both Dixon plots (Figure S1) indicated that PZA and POA are mixed inhibitors with Ac-p53 and, consequently, both can bind the enzyme in the presence and absence of the Ac-p53 substrate. Next, with the substrate Ac-p53 concentration fixed and the cofactor (NAD+) concentration varying, substrate saturation curves for PZA and POA were constructed to study in greater detail the nature of their interactions relative to the cofactor NAD⁺. The data was fitted to the different inhibitory models. By using nonlinear least-squares analysis (Figure S1), the inhibition model that was a better fit for the saturation curves was selected. In these analyses, PZA displayed mixed inhibition with NAD+, whereas POA appeared to inhibit SIRT6 in a noncompetitive manner. Hence, the presence of NAD⁺ is required only for the binding of POA, but not of PZA. This result was further explored by using STD NMR spectroscopy.

NAD+, NAM, and PZA bind reversibly to SIRT6

The reversibility and binding orientation of the ligands NAD⁺, NAM, POA, and PZA, were determined individually in solution

in the presence of SIRT6 by using STD NMR titration. This NMR technique is used to identify the motifs of ligands that are in direct contact with a protein. Those are the ligands that exhibit the highest degree of saturation and show the most intense NMR signals in an STD spectrum. Comparison of the STD responses for various protons of a ligand enabled Mayer and Meyer to develop a group epitope mapping protocol for determination of the relative orientation of bound ligand in solution. [19]

Observation of the NAD $^+$, NAM, and PZA signals in the STD spectra (Figure 2A–C) established that these compounds interact with SIRT6, with the bound and free states in fast exchange on the NMR time scale. However, resonances attributed to POA were not observable in the STD spectra at SIRT6/POA ratios below 1:100 and were negligible above this ratio (Figure 2D). This finding is consistent with slow exchange (tight binding) or non-specific enzyme interactions. However, slow exchange is not consistent with the kinetics and IC $_{50}$ data, and competition experiments with NAD $^+$ were used to better understand this observation.

Individual titration of SIRT6 with NAM and with NAD⁺ served not only as a positive control but also enabled interrogation of SIRT6 interactions with these two ligands. Despite extensive studies on the effect of NAM on sirtuin deacylase activity, the mechanism of inhibition of SIRT6 by NAM is not fully understood. In our studies, STD NMR complemented fluorescence enzyme assays. NMR shed light on the dynamics of NAM and NAD⁺ binding to SIRT6. Not only was the reversible binding of NAM and NAD⁺ confirmed, but NAM and NAD⁺ binding geometries were suggested based on the percentage enhancement of individual proton resonances. The percentage enhancement, or relative STD effect, a quantification of the STD effect according to Mayer and Meyer's protocol, was determined from Equation (1).^[19] The percentage attributed to each proton is indicated on the chemical structures (Figure 2 A–D).

$$STD = \frac{I_{STD}}{I_0} \tag{1}$$

In Equation (1), the term $I_{\rm STD}$ is the integral of a single proton resonance in the STD spectrum. This term corresponds to the difference (I_0 – $I_{\rm SAT}$), where I_0 is the integral of that unsaturated proton (reference spectrum), and $I_{\rm SAT}$ is the integral of the same proton after saturation (spin-saturated spectrum). The integrals ($I_{\rm STD}$) are referenced to the respective unsaturated spectrum. Subsequently, each STD value is normalized to the proton resonance with the largest STD effect to obtain the percentage enhancement or relative STD effect. [20]

NAM, PZA, and POA binding affect NAD+ binding

Titration of the enzyme–NAD⁺ complex with the three ligands NAM, PZA, and POA elucidated specific ligand–SIRT6 binding requirements, the relative affinities of these compounds for the enzyme, and the response of the enzyme to ligand complexation. In this experiment, the contrast in resonance intensity attributable to enzyme-complexed species with the signals

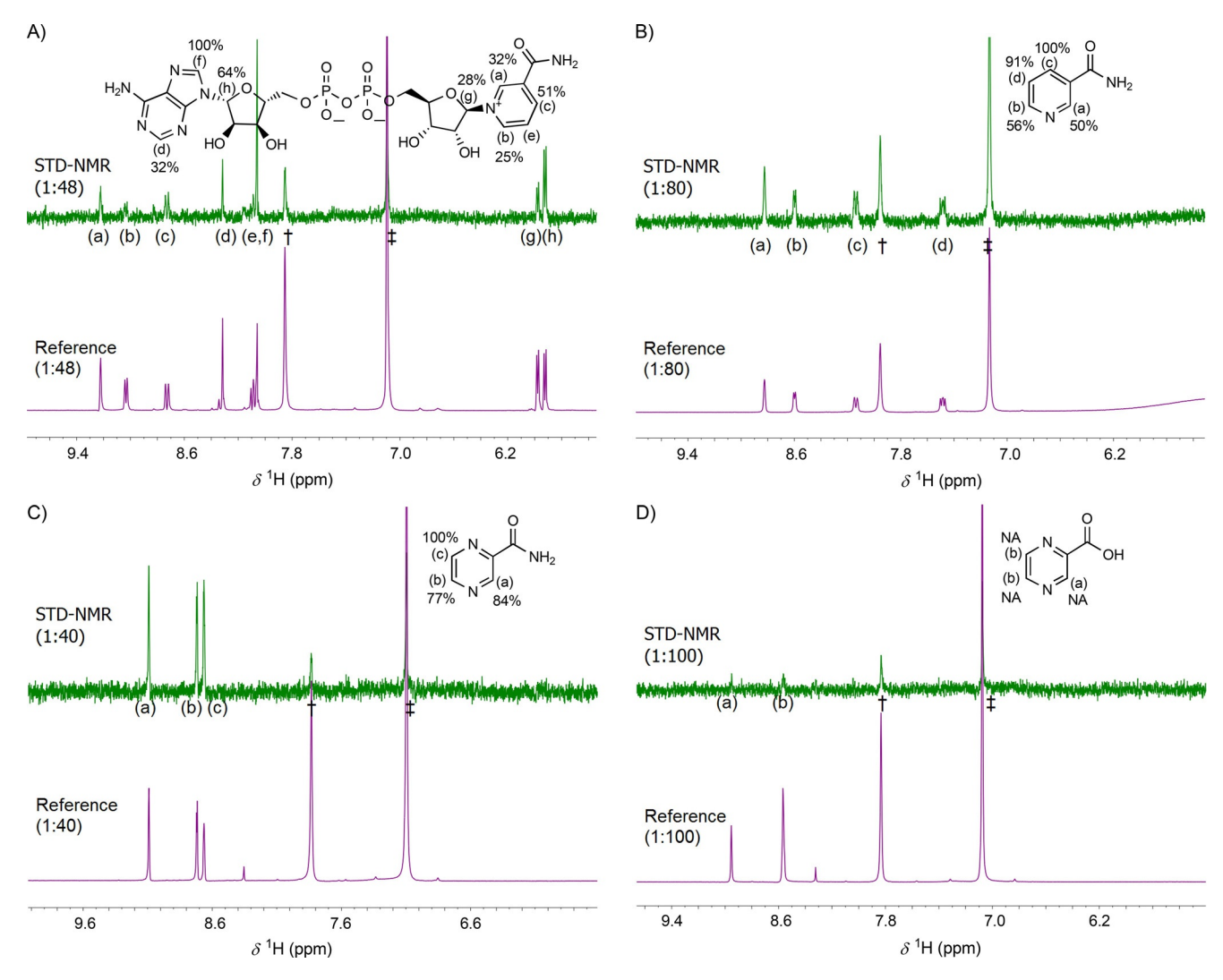


Figure 2. Relative STD effects. Expansion of reference 1D 1 H NMR and STD NMR spectra of: A) NAD $^{+}$, B) NAM, C) PZA, and D) POA in the presence of SIRT6 at 400 MHz and 298 K. Ratios correspond to the excess of ligand to enzyme. The percentage assigned to each proton resonance corresponds to the percentage of enhancement, which is indicative of the proximity of each proton to the enzyme. These values were calculated by integration of individual signal intensities (l_{STD}) in the STD spectrum and individual intensities (l_{O}) in the reference 1D-NMR spectrum. The ratios of the intensities were normalized by using the largest STD effect as a reference. Contribution from resonance e of NAD $^{+}$ was not assigned, as this resonance overlapped with resonance h in the reference and STD spectra. † and \pm correspond to peaks from the residual amount of imidazole used in purification of the enzyme. Note that the spectra are not on the same scale (as indicated by the noise).

of the dissociated species at increasing ligand concentrations illustrates binding dynamics. On titration of the three ligands, quantification of the integrals in the reference spectra (I_0) as well as in the STD spectra (I_{STD}) allowed determination of the STD amplification factor (A_{STD}), $^{[19]}$ as defined in Equation (2). The A_{STD} is the effective magnitude of the ligand proton STD signal relative to the magnitude of a proton resonance in the protein. $^{[20]}$ The A_{STD} values permit identification of small molecule–enzyme contacts, to include recognition of the disturbance or reinforcement of those interactions by other ligands or substrates in a dynamic environment.

$$A_{\text{STD}} = \left(\frac{I_{\text{STD}}}{I_0}\right) \times \left(\frac{[L]_{\text{total}}}{[P]_{\text{total}}}\right) = \text{STD} \times \text{ligand excess}$$
 (2)

In this series of titration experiments, the concentration of the enzyme and the cofactor NAD $^+$ was fixed. The molar ratio of SIRT6 to NAD $^+$ was 1:48 in each case. The holoenzyme was titrated independently with each ligand, and the $A_{\rm STD}$ value of each NAD $^+$ resonance, and of each ligand resonance, was monitored at each titration point (Figure 3 A–C). The percentage of enhancement was also determined. For simplicity, the $A_{\rm STD}$ values of three select NAD $^+$ resonances were plotted against ligand concentration; all the $A_{\rm STD}$ values of NAM, PZA, and POA were shown (Figure 3 A–C). These curves reflect the difference in the degree of saturation of the bound molecules.

As suggested by the decreasing trend in the A_{STD} values of the NAD⁺ proton resonances, the three inhibitors were able to disrupt the contacts made by the NAD⁺ protons with the enzyme residues. In Figure 3E the percentage enhancement of NAD⁺ is illustrated before and after addition of NAM, PZA,

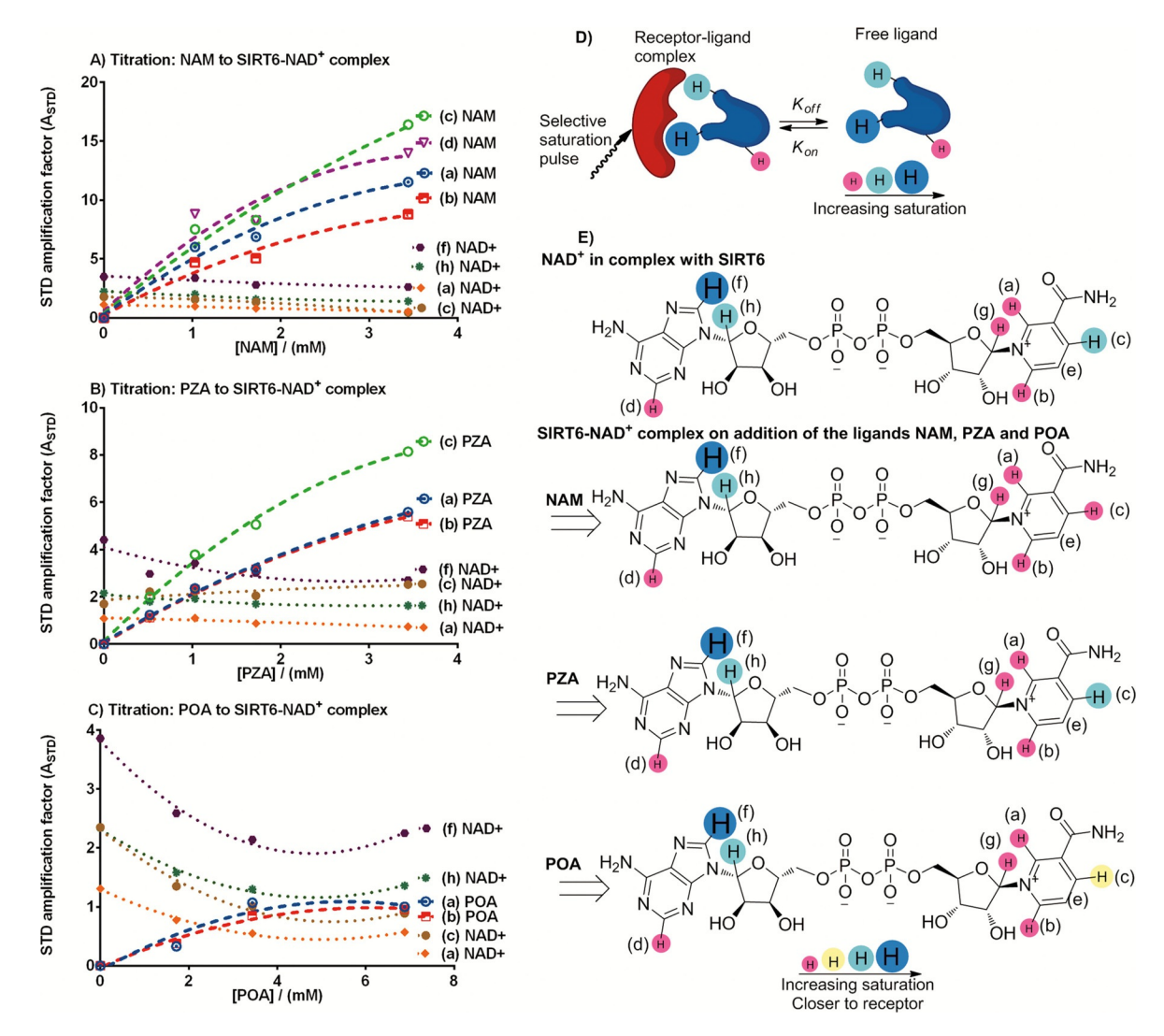


Figure 3. Diagrams showing the STD amplification factors (A_{STD}) of selected NAD⁺ resonances (....), determined from STD spectra from titration of the ligands A) NAM, B) PZA, and C) POA (----) to the SIRT6–NAD⁺ complex at a fixed enzyme/cofactor ratio of 1:48. The trend of the A_{STD} values of the corresponding proton resonances (of titrated and fixed substance) indicates the enhancement or disturbance of the occurring interaction with the enzyme. D) Scheme summarizing the STD-NMR experiments. The closer the protons are to the enzyme the more saturation they receive, represented by the size of the spheres. E) Representation of the binding pose of NAD⁺. The structures qualitatively summarize the variation in the proximity of individual NAD⁺ protons to the enzyme before and after addition of each ligand. The size and color of the spheres only appear altered when the corresponding ligand changes the enhancement of a particular NAD⁺ resonance on the enzyme–cofactor complex. The smaller the spheres become, the further the protons are pushed away from the enzyme. The purine moiety appears barely affected in the NAM and POA cases, whereas the NAM purine is affected; this suggests that these two molecules disturb the NAM moiety site most.

POA. The protons of NAD⁺ are represented by circles. The first structure in Figure 3E gives a qualitative idea of the proximity of each NAD⁺ proton in the SIRT6–NAD⁺ complex, as assessed by the intensity of the resonance. The three subsequent structures illustrate the change in the enhancement of each NAD⁺ proton resonance relative to the initial most intense resonance upon addition of each ligand to the holoenzyme. With the exception of proton c, in each case, the change in the relative STD effect for most protons was minimal and remained within the same range; for that reason, the size of most circles appear unchanged in Figure 3E. A small reduction in the relative STD effect was observed throughout the molecule. This decrease could be the result of secondary site occupancy, and therefore an overall rearrangement of the enzyme structure.

However, NAM and POA were able to alter the proximity of the NAM moiety of NAD⁺ to the enzyme at proton c, whereas PZA had no effect (Figure 3 E). This finding suggests a difference in the binding pose of PZA relative to NAM and POA, despite the structural similarities of these small ligands. Interestingly, in this experiment, POA resonances were observable in the STD spectra. This is the first evidence that POA is able to bind the holoenzyme at an allosteric site.

NAD+ concentration affects ligand affinity

To investigate the effect NAD⁺ has on the binding poses of NAM, PZA, and POA, titration of these three SIRT6–ligand complexes with increasing concentrations of NAD⁺ was studied. In

www.chembiochem.org

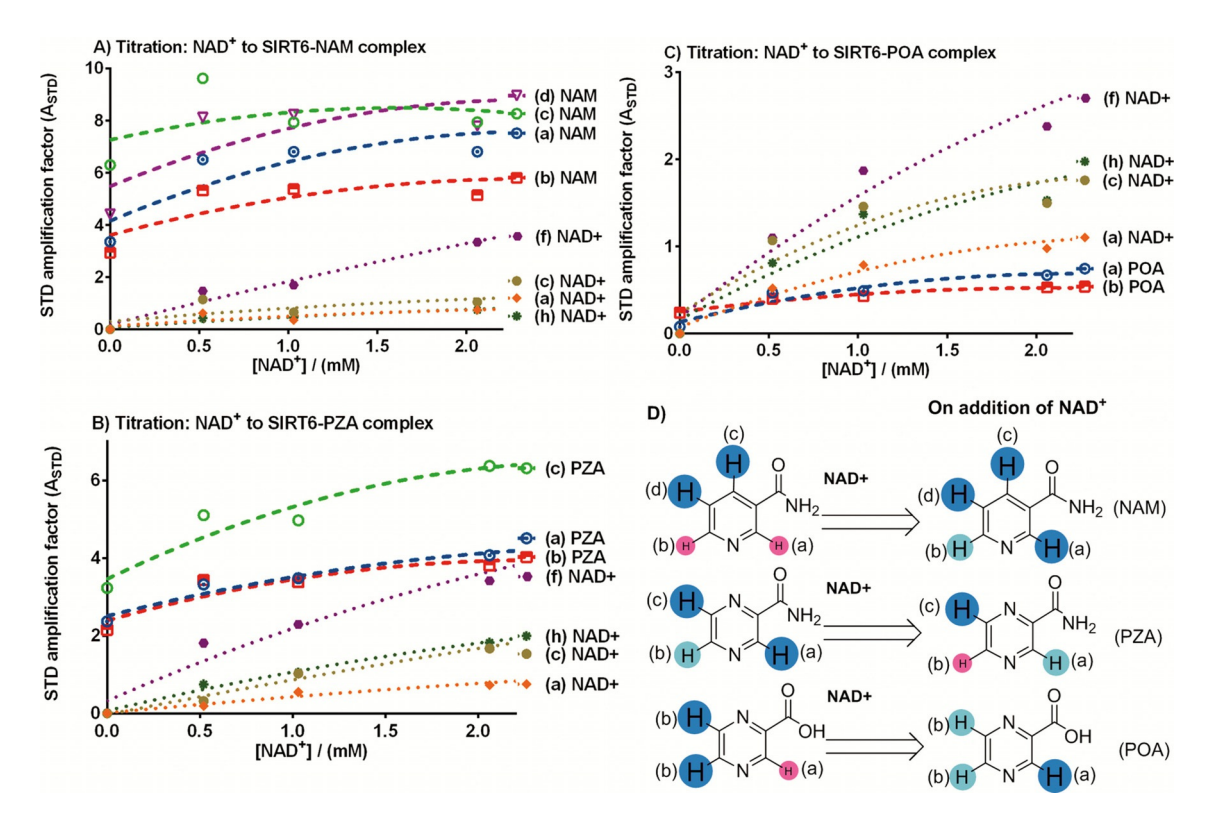


Figure 4. Diagrams showing the STD amplification factors (A_{STD}) of proton resonances corresponding to each ligand (----): A) NAM, B) PZA, and C) POA in complex with SIRT6 on titration of NAD⁺ (····). The trend of the A_{STD} values of the corresponding proton resonances (titrated and fixed substance) indicates the enhancement or disturbance of the interaction with the enzyme. D) Representation of the binding pose of each ligand before and after addition of the cofactor NAD⁺. The size of the spheres is based on the percentage of enhancement and indicates the relative proximity of the proton resonances of each ligand complexed with SIRT6 before and after addition of the cofactor NAD⁺. The smaller the spheres become, the further the protons are pushed away from the enzyme relative to the strongest interaction stablished. Conversely, the bigger the spheres, the stronger the interaction.

these competition experiments, the $A_{\rm STD}$ value of each ligand proton resonance was monitored upon formation of the enzyme–ligand complex, and upon addition of cofactor NAD $^+$. The molar ratio of SIRT6 to each ligand was fixed at 1:40. The $A_{\rm STD}$ values of each ligand resonance and of the three NAD $^+$ resonances were plotted against the concentration of NAD $^+$ (Figure 4A–C).

Titration of the NAM–enzyme complex with NAD⁺ led to an increase in the intensity of most NAM STD resonances, despite an unchanging concentration of NAM. The greatest effect was observed at protons a and d, as indicated by the positive trend of these two curves; with proton c, the opposite effect was observed (Figure 4A).

Furthermore, addition of NAD⁺ to the PZA–SIRT6 complex also resulted in an increase in the intensity of the STD resonances of PZA, with resonances a and b least affected (Figure 4B). Proton resonance c of PZA, which originally was the closest to the enzyme, remained in close proximity of the enzyme–NAD⁺ complex, as can be seen in Figure 4B. The POA resonances were nearly undetectable prior to NAD⁺ addition, especially resonance a. Upon addition of NAD⁺ to the POA–SIRT6 complex, resonance a grew more rapidly than resonances b, which were attributed to the two nearly magnetically equivalent protons (Figure 4C). In summary, the three inhibitors displayed a higher affinity for the SIRT6–NAD⁺ complex than for the apo-

enzyme, based on the positive slopes of the ligand A_{STD} values. The positive slope of the curves indicated that tighter interactions between SIRT6 and the ligands occurred with increasing NAD⁺ concentrations.

Variation in the percentage enhancement received by NAM, PZA, and POA is depicted in Figure 4D. In the initial structures, the size of the circles qualitatively represents the proximity of the proton resonances of each ligand to SIRT6 before addition of NAD⁺. Upon addition of NAD⁺, the percentage enhancement of at least one proton resonance of each ligand was significantly augmented, by not less than onefold (Figure 4A-C and Supporting Tables). The most profoundly influenced resonance for each ligand was resonance d for NAM, resonance c for PZA, and resonance a for POA. Therefore, the size of the circles in the structures upon addition of NAD⁺ represents the recalculated percentage enhancement relative to the former most intense resonance, thus establishing a consistent comparator. This illustration suggests new binding poses were adopted by each of the three ligands upon addition of NAD⁺. Altogether, the increase in A_{STD} values and the percentage enhancement of the ligands upon addition of cofactor NAD+ suggest that the enzyme undergoes a major rearrangement. Binding of the cofactor that drives those changes consequently influenced the binding poses of the three ligands examined.





NAD⁺ interacts with SIRT6 mainly through the adenine moiety

Titration experiments with NAD⁺ alone suggested that binding of the NAD+ cofactor in the absence of a substrate such as Acp53 is governed by interactions between the adenine moiety and SIRT6 (see enhancement of proton f resonance; Figure 2 A). The significant difference observed in the calculated fractional enhancement of other proton resonances relative to proton f indicates that proton f is nearest to the enzyme. Proton h appears to be the second closest to SIRT6, as would be consistent with the NAD+ structure. The tighter interaction between SIRT6 and the purine moiety of NAD+, rather than the pyridine ring, was anticipated by X-ray diffraction studies.[21] Avalos reported that "nonproductive" and "productive" conformations were common among NAD+-complexed sirtuin orthologues. The productive conformation, observed upon binding of an acetylated substrate and NAD+, places the NAM moiety of NAD⁺ in a highly conserved pocket (pocket C).^[21] In this conformation, similar enhancement factors for the proton resonances of both the purine and pyridine moieties are expected. The failure of the NAM moiety to dock in pocket C of SIRT6 upon refolding could be a consequence of the absence of acetylated substrate (Ac-p53).[21] Alternatively, the lack of a conserved cofactor-binding loop in SIRT6 might prohibit the assumption of the productive conformation, even in the presence of acetylated substrate.

The replacement of the loop by an ordered helix, the absence of a helix bundle in the small domain, and the loss of a salt bridge renders SIRT6 flexible. This flexibility contributes to the positioning of the zinc-binding domain with respect to the Rossmann fold and substrate-binding site. Failure of the necessary reorganization to occur absent the peptide substrate might account for the diminished pyridine resonance intensities.

STD NMR competition experiments in which a fixed concentration of Ac-p53-SIRT6 was titrated with increasing NAD+ concentrations and, vice versa, where a fixed concentration of NAD⁺-SIRT6 was titrated with increasing concentrations of Acp53, helped to determine whether the absence of the substrate Ac-p53 or the structural differences between SIRT6 and other sirtuins were responsible for the binding conformation of NAD⁺. No difference in the STD enhancement of the NAD⁺ proton resonances was revealed. This finding confirmed that the productive conformation observed with other sirtuins was not observed with SIRT6, [22] at least not upon binding of acetylated substrate (Figures S3 and S4). In addition, the failure to assume the postulated productive conformation affords a rationale for the less stable substrate-protein interaction, and hence the poor deacetylase activity of SIRT6. Further conformational changes might be required for the sufficiently tight substrate-cofactor interactions that facilitate SIRT6 deacetylase activity.

NAM binds in the absence of the cofactor NAD+

Titration of NAM with SIRT6 alone showed that NAM bound the enzyme in the absence of the acetylated peptide and the NAD⁺ cofactor (Figure 2B). NAM docks in the conserved pocket C of various sirtuin orthologues through hydrogen bonding interactions of the carboxamide. A low-energy conformation in which the carboxamide and the pyridine ring bind in a nearly coplanar manner occurs in the non-productive conformation. A less favorable out-of-plane rotamer is found in the recognized productive sirtuin-NAD+ complex.[21] In the present work, there is a marked difference between enhancement of the resonances of proton pair c and d and pair a and b of NAM that is consistent with the NAM ring not sitting flat in the binding pocket. The lower enhancements observed for the protons next to N1 of the pyridine ring, that is, resonances a and b, suggest a weaker interaction between N1 and the enzyme. Moreover, the similar and greater enhancement of resonances c and d, the protons adjacent to the carboxamide group, is consistent with NAM being anchored to the C pocket through the carboxamide with the perpendicular pyridine ring placing the protons near N1 further from the pocket. Neither substrate nor cofactor was present in this experiment. Consistent with SIRT6 possessing unique structural features and utilizing a different binding mechanism, NAM displayed conformational differences when bound to SIRT6 in contrast to binding to other sirtuins.

NAM competes with the NAD+ pyridyl moiety

Titration of the NAD $^+$ -enzyme complex with NAM disrupted SIRT6–NAD $^+$ interactions. The NAD $^+$ A_{STD} values were attenuated with increasing concentrations of NAM (Figure 3 A). The NAD $^+$ resonances most affected were the pyridyl protons a, b, and c, despite being the weakest interactions. This specificity suggests that NAM competes with the pyridyl moiety of NAD $^+$ for binding.

Titration of the NAM-enzyme complex with NAD⁺ (Figure 4A), on the other hand, led to a selective increase in enhancement of the NAM resonances upon NAD+ binding. The A_{STD} values of proton resonances a and d increased, whereas that of proton c, the proton in closest proximity to the enzyme in the absence of NAD+, decreased but stayed within the same range. The NAM resonances in the presence of NAD⁺ reached a similar percentage enhancement, suggesting a similar proximity of the four proton resonances to the enzyme (see proposed binding pose of NAM in Figure 4D). This change in the NAM binding pose might be a consequence of SIRT6 promotion of pyridyl rotation about the carboxamide group induced by NAD⁺ binding, placing all of the protons a similar distance from the enzyme. NAM-induced configurational changes were likely related to reactivity, as observed previously with other sirtuin isoforms.^[21]

The binding of NAM to the SIRT6–NAD⁺ complex, as well as to SIRT6 alone, and the greater affinity of NAM for the former, is consistent with mixed inhibition relative to cofactor NAD⁺. Moreover, the changes observed in both STD NMR competition





experiments (addition of NAD⁺ to the SIRT6–NAM complex and addition of NAM to the SIRT6–NAD⁺ complex) suggest a mutual allosteric effect.^[23]

PZA binds SIRT6 in the absence of NAD+ and Ac-p53

The mixed inhibition of SIRT6 relative to NAD⁺ or Ac-p53 that was proposed from kinetics studies was confirmed by STD NMR. PZA bound both the SIRT6-NAD+ complex and SIRT6 alone; however, the STD effect and, consequently, the amplification factor (A_{STD}) observed for the three PZA proton resonances, was higher (Figure 4B), and the binding pose of PZA changed (Figure 4D) in the presence of NAD+. The similar enhancements of PZA proton resonances a, b, and c of 84, 77, and 100%, respectively, in the absence of NAD+, and the distinct recalculated enhancements of 75, 55, and 100% when NAD+ was present suggested that an enzyme rearrangement took place. Hence, protons a and b were pushed away from the enzyme, but the interaction with proton c was enhanced. Lastly, proton c, contiguous to N1 in the pyrazine ring, had the largest A_{STD} value in both cases and therefore was in closest proximity to SIRT6, suggesting that, like NAM, PZA might be anchored to the enzyme through the carboxamide group.

PZA binds more tightly than NAM to the holoenzyme

Titration of the SIRT6-NAD+ complex with PZA resulted in reduction of NAD $^+$ A_{STD} values (Figure 3B). In contrast to NAM, PZA proportionally disturbed all of the NAD⁺ protons that interact with SIRT6 (as reflected by the decrease in the A_{STD} values); this indicated that PZA likely does not bind at the NAM binding site, but rather disrupts NAD⁺ binding through a second regulatory site. Despite the structural similarity between NAM and PZA, these two compounds make contacts with the enzyme and enzyme-NAD+ complex through different protons and in different conformations (Figure 4D). On the other hand, titration of the SIRT6-PZA complex with NAD⁺ increased the saturation PZA receives from the enzyme (Figure 4B). The increase in the A_{STD} values, despite the constant PZA concentration, suggested that the binding of NAD⁺ to SIRT6 induced a conformational rearrangement. Unlike NAM, upon titration of the SIRT6-PZA complex with NAD+, proton c became the closest to the SIRT6-NAD+ complex, whereas the A_{STD} values of protons a and b stayed within the same range. Presumably, protons a and b were pushed away, as reflected in the recalculated percentage enhancement. In the resulting conformation, the A_{STD} values and percentage enhancement of PZA suggested that the protons no longer had the same proximity to SIRT6, revealing the importance of the substitution of C4 of the pyridine ring by N1 of the pyrazine, where the adjacent proton becomes the closest to the enzyme (proposed conformation in Figure 4D). Ultimately, competition experiments between NAM and PZA revealed no difference in the A_{STD} values when PZA was added to the NAM-SIRT6 complex or when the PZA-SIRT6 complex was titrated with increasing concentrations of NAM (Figure S2). This result again suggested that PZA and NAM bind different sites.

POA binds SIRT6 non-specifically in the absence of NAD+

In contrast to PZA and NAM, POA did not bind SIRT6 at enzyme/ligand stoichiometries below 1:100, as observed in Figure 2D. The intensity of resonances attributed to POA were very weak, even at very high enzyme/ligand ratios. As STD NMR is only suitable for binding affinities within the micromolar to the millimolar range, failure to detect STD resonances of POA could be rationalized by either a very high enzyme affinity^[19,24] or the absence of association with the enzyme. Unfortunately, high affinity as a rationale is not consistent with the enzyme kinetics and IC₅₀ data (Table 1). Resonances observed at such ligand excesses are most likely a consequence of nonspecific enzyme interactions. We speculate that the failure to detect resonances was the result of an uncompetitive inhibition process, as suggested by the kinetics experiments with POA and NAD⁺ described earlier (Figure S1). As a consequence of this assumption, no POA STD signals are expected in the absence of NAD⁺.

POA binds SIRT6 only in the presence of NAD+

NAD $^+$ is essential for binding of POA, whereas the presence of the p53 peptide is not. The addition of NAD $^+$ to the POA–SIRT6 complex revealed the previously undetectable resonances of POA (Figures 3 C and 4 C). The intensity of the resonance attributed to the POA proton a, adjacent to the carboxylic acid group, increased more rapidly than resonances b, attributed to the two protons that were nearly magnetically equivalent. Increasing amounts of POA were also capable of displacing NAD $^+$ from the binding site, as POA binding was accompanied by a decrease in the $A_{\rm STD}$ values of NAD $^+$ (Figure 3 C).

Conclusion

Determination of binding modes is important for revealing the mechanistic differences between inhibitors and the interaction of those inhibitors with various sirtuins. To date, crystallographic structural analysis of sirtuin binding sites has exposed a rationale for differentiation of the binding affinities of various sirtuins. STD NMR spectroscopy was used to interrogate the SIRT6 catalytic process and to complement fluorescence enzyme assay kinetics studies. These experiments not only suggested the mechanism by which the enzyme is regulated, but also illustrated the interactions between the studied ligands and enzyme. These investigations illuminated how the interactions with the enzyme affect substrate and cofactor enzyme affinity at the atomic level. Our findings are not limited to observance of competition between ligands or displacement of one molecule or the other but rather to atomic details of the enhancement or disruption of the ligand/substrate/cofactor interaction with the enzyme. Our data established that NAD+ increased the affinity for the ligands under study (NAM, PZA, and POA), but at the same time, these ligands were dynamically able to disturb the NAD⁺-enzyme interactions by displacing the NAD+ pyridyl moiety in the cases of NAM and POA, and by displacing the entire NAD⁺ molecule in the case of PZA.



PZA and POA were mixed inhibitors of SIRT6 against the acetylated substrate used in this study (Ac-p53). However, when PZA and POA were tested against the cofactor NAD+, the enzyme was inhibited in a mixed and an uncompetitive fashion, respectively. These findings were later confirmed by STD NMR spectroscopy, in which binding to the apoenzyme was observed with NAM and PZA but not with POA. As PZA and POA inhibited the enzyme by a mixed mechanism relative to Ac-p53, presence of this substrate was not required for binding of either compound. However, it is known that the catalytic efficiency of SIRT6 appears to be dependent on the nature of the substrate. Recent data have shown that fatty-acylated Lys substrates are more efficiently deacylated by SIRT6 than acetylated substrates.[11,25] Consequently, we anticipate a different inhibitory constant for PZA, POA, and PZA analogues upon binding to SIRT6 when long chain fatty-acylated substrates are present. Conversely, the PZA mixed and POA uncompetitive inhibition of SIRT6 relative to NAD+ suggest that catalysis is dependent upon and is highly regulated by NAD+ binding. Overall, NAD+ promotes very specific interactions, highlighting the importance of NAD⁺ to the catalytic action of SIRT6. Given the role of the substrate on efficiency and the role of the cofactor on enzyme conformation, SIRT6 appears to have high selectivity and specificity.

Despite the similarities between POA and NAM or PZA, POA clearly interacts with SIRT6 through a different mechanism, uncompetitive relative to NAD $^+$, with PZA and POA IC $_{50}$ values in the high micromolar range (Table 1), suggesting a weak interaction. Guided by our binding studies, the IC $_{50}$ values might be improved by rational modifications to the pyrazine scaffold, as observed with 5-MeO-PZA and 5-CI-PZA (Table 1). Furthermore, these studies bring additional insights into how PZA and POA affect the functionality and conformation of the enzyme. These insights are relevant not only for the identification of efficient inhibitors, but also for recognition of new roles for PZA in treatment.

The role of the acetylated substrate on the enzyme's conformation was investigated by competition STD NMR experiments between the acetylated peptide (Ac-p53) and NAD+. The absence of change in the intensities of the NAD⁺ resonances upon titration of Ac-p53 suggests that at least this particular substrate does not influence SIRT6 catalytic activity or configuration of the enzyme. This could offer a rationale for the poor deacetylase activity SIRT6 displays, as well as the shortage of potent SIRT6 inhibitors. The failure of the simpler, lower molecular weight peptides to bind tightly suggests an explanation for the lack of binding site saturation by the acetylated peptide (H3K9Ac) by isothermal titration calorimetry described by Pan et al. [22] Alternatively, other conformational changes might be required for promotion of the interaction between the cofactor and the substrate to facilitate the deacetylase activity of SIRT6. It appears that the hydrophobic tail of fatty-acylated substrates could cause conformational changes required for catalysis. Alternately, hydrophobic interactions of fatty acyl substrate might be required for substrate-cofactor interactions, especially to overcome the rigidity conferred to SIRT6 by the absence of a flexible NAD⁺ binding loop.

The greater affinity of SIRT6 for longer acylated chains and the increased catalytic efficiency [11,26] could be a consequence of more drastic conformational rearrangements when SIRT6 binds with higher affinity to a substrate. To test this hypothesis, competition STD NMR will be used to explore the interactions of a fatty-acylated lysine substrate such as TNF- α K-20 with sequence Ac-EALPK(MyrK)^[26] and NAD+ with SIRT6.

Experimental Section

Chemicals and reagents: Nicotinamide (99%) was purchased from Alfa Aesar. Pyrazinamide (99%), pyrazinoic acid (99%), β-Nicotinamide adenine dinucleotide hydrate (NAD $^+$, > 96.5%), dimethyl sulfoxide (DMSO), and tergitol solution (type NP-40, 70% in H $_2$ O) were purchased from Sigma–Aldrich. [D $_6$]DMSO (99.9%) was purchased from Cambridge Isotope Laboratories. Deuterium oxide (D $_2$ O, 99.92%) was purchased from Medical Isotopes, Inc. [D $_{10}$]-DL-Dithiothreitol ([D $_{10}$]DTT, 98%) was purchased from Isotec. Lysozyme and isopropyl-D-thiogalactopyranoside (IPTG) were purchased from LabScientific, Inc. [D $_8$]Glycerol was prepared according to Koch et al. [27] Acetylated peptide Arg-His-Lys-Lys $^{\rm Ac}$ (> 96%) and fluoroacetylated peptide Arg-His-Lys-Lys $^{\rm Ac}$ -AMC (> 91%) were purchased from China Peptides Co. Ltd.

Preparation of SIRT6 for kinetics and STD NMR studies: Histagged SIRT6, cloned into the bacterial expression vector pQE-80, was purchased from Addgene (plasmid 13739). Plasmid DNA was extracted and transformed into Escherichia coli BL21-DE3 cells. The transformed bacterial cells were grown at 37 °C in LB medium with 100 μg per mL of ampicillin, expression was induced with IPTG (1.0 mM) at an OD₆₀₀ of 0.6–0.8, and the cells were allowed to grow for an additional 12 h. Harvested cells were resuspended in lysis buffer (sodium phosphate buffer (50 mм), pH 7.2, NaCl (250 mм), imidazole (5 mm), and β -mercaptoethanol (1 mm)), and lysed by using 2% tergitol-type NP-40 and lysozyme (1 mg mL⁻¹). Cell debris was removed by 30 min centrifugation at 4°C and 21 000 rpm in a JA-25.5 rotor. The supernatant was incubated with Ni-NTA resin for 1 h at 4°C. Flowthrough, wash, and elution fractions were collected according to the Qiagen protocol for purification of His₆-tagged proteins from E. coli under native conditions (QIAexpressionist). Fractions were analyzed by SDS-PAGE and western blotting, and elution fractions containing purified SIRT6 were pooled. By using Amicon Ultra centrifugal filters with MWCO 10 kDa (Millipore), the elution fractions were transferred into storage buffer for fluorimetric assays (sodium phosphate buffer (50 mm) pH 7.2, NaCl (20 mm), β -mercaptoethanol (1 mm), and 20% glycerol) and storage buffer for STD NMR assays (Tris·HCl buffer (50 mm) pH 8.0, NaCl (137 mm), KCl (2.7 mm), MgCl₂ (1.0 mm), and 6% [D₈]glycerol in D₂O), accordingly. Enzyme concentrations were determined by using the Bradford method with bovine serum albumin (BSA) as the standard.

Measurement of deacetylation activity and kinetics of inhibition by using a fluorescent peptide: Inhibitory constants (K) and IC₅₀ values were determined under saturating substrate conditions by using a fluorimetric assay (components were purchased separately). This assay system allows detection of a fluorescent signal upon SIRT6 deacetylation of the fluorescent substrate peptide (AMC-p53) with amino acids 379–382 (Arg-His-Lys-Lys^{Ac}). Sirtuin deacetylation of the substrate renders the fluorophore–substrate bond susceptible to treatment with lysyl endopeptidase. Trypsin cleavage releases the fluorophore, resulting in an increase in fluorescence. Fluorescence intensity was measured on a Synergy HT Multi-Mode mi-



croplate fluorescence reader. K_i values, IC_{50} values, and modes of inhibition were determined by using Dixon's methodology with varying concentrations of the acetylated substrate peptide. The best fit models were verified at varying concentrations of NAD⁺ by using Prism GraphPad software.

STD NMR studies: Samples were prepared in Tris·HCl buffer, pH 8.0 (50 mm, 0.5 mL with 6% [D₈]glycerol, NaCl (137 mm), KCl (2.7 mm), [D₁₀]DTT (1 mm), and 99% D₂O). Enzyme concentrations in the NMR samples ranged between 20 and 40 μ m; ligands concentrations ranged from 0.08 to 11 mm. Saturation curves were constructed with enzyme-to-ligand molar ratios ranging from 1:2 to 1:275.

STD spectra were collected by using the standard pseudo-2 \mbox{D} pulse sequence, STDDIFFESGP.3, with 32 K data points, 1024 transients, and 32 stationary scans. STD NMR spectra were recorded on a Bruker Avance 400 MHz spectrometer equipped with a common probe and a relaxation delay of 3.1 s. Data processing was performed on a PC with Bruker Topspin v2.1 software. A train of selective Gaussian-shaped pulses $(\gamma^*(B_1/2\pi) = 86 \text{ Hz})$ of 50 ms duration with a 100 µs delay between each pulse was used to saturate protein signals. The total saturation time was set to 3.0 s. The proton carrier was placed at 0.79 and 40 ppm for on- and off-resonance saturation, respectively. The on- and off-resonance experiments were recorded in an interleaved fashion to avoid any experimental inconsistencies and minimize the effect of any radiofrequency induced by sample temperature changes. A gradient spoil sequence with smsq10.100 pulses of 3 and 1 ms was utilized to destroy unwanted magnetization. To enhance selective observation of ligand resonances, a transverse relaxation filter (T1p) of 10 ms was applied. This filter eliminated the rapidly relaxing receptor resonances, suppressing protein background and therefore facilitating analysis. As very low concentrations of ligands were used, the residual H₂O signal was suppressed according to the excitation sculpting method with gradients by Hwang et al. [28] The residual HDO signal was effectively suppressed with Squa100.1000-shaped pulses of 2 ms.

Acknowledgements

We thank Dr. Donna Baldisseri (Bruker BioSpin Corporation) for her help with the STD-NMR experiments and for providing us with the stdsplit 1.3 program to identically process and subtract the spectra, avoiding artifact signals. We are grateful to Dr. Mike Lumsden (Dalhousie University) and Dr. Glenn A. Facey (University of Ottawa), for helpful conversations and advice on NMR spectroscopy. Data visualization was aided by Daniel's XL Toolbox add-in for Excel, version 6.70, by Daniel Kraus, Würzburg, Germany (www.xltoolbox.net). This work was supported by the National Institutes of Health (NIH) AIDS Clinical Trial Group Network, Brigham and Women's Hospital (grant ACTG-108402).

Conflict of Interest

The authors declare no conflict of interest.

Keywords: NAD $^+$ · nicotinamide · pyrazinamide · SIRT6 · STD-NMR

- [1] a) P. A. Marks, T. Miller, V. M. Richon, *Curr. Opin. Pharmacol.* **2003**, 3, 344–351; b) Y. Dai, D. V. Faller, *Transl. Oncogenomics* **2008**, 3, 53–65.
- [2] M. D. Parenti, S. Bruzzone, A. Nencioni, A. Del Rio, Mol. Biosyst. 2015, 11, 2263 – 2272.
- [3] H. Yuan, R. Marmorstein, J. Biol. Chem. 2012, 287, 42428-42435.
- [4] S. R. Kim, K. S. Lee, S. J. Park, K. H. Min, Y. H. Choe, H. Moon, W. H. Yoo, H. J. Chae, M. K. Han, Y. C. Lee, J. Allergy Clin. Immunol. 2010, 125, 449 – 460.
- [5] D. J. Lomb, G. Laurent, M. C. Haigis, Biochim. Biophys. Acta Proteins Proteomics 2010, 1804, 1652 – 1657.
- [6] a) A. A. Sauve, Biochim Biophys. Acta 2010, 1804, 1591–1603; b) L. Lafon-Hughes, M. V. Di Tomaso, L. Mendez-Acuna, W. Martinez-Lopez, Mutat. Res. 2008, 658, 191–214; c) J. L. Feldman, K. E. Dittenhafer-Reed, J. M. Denu, J. Biol. Chem. 2012, 287, 42419–42427.
- [7] C. Y. Liao, B. K. Kennedy, Cell Res. 2012, 22, 1215-1217.
- [8] G. Liszt, E. Ford, M. Kurtev, L. Guarente, J. Biol. Chem. 2005, 280, 21313– 21320
- [9] a) P. Kokkonen, M. Rahnasto-Rilla, P. H. Kiviranta, T. Huhtiniemi, T. Laitinen, A. Poso, E. Jarho, M. Lahtela-Kakkonen, ACS Med. Chem. Lett. 2012, 3, 969–974; b) E. Michishita, R. A. McCord, E. Berber, M. Kioi, H. Padilla-Nash, M. Damian, P. Cheung, R. Kusumoto, T. L. Kawahara, J. C. Barrett, H. Y. Chang, V. A. Bohr, T. Ried, O. Gozani, K. F. Chua, Nature 2008, 452, 492–496; c) T. L. Kawahara, E. Michishita, A. S. Adler, M. Damian, E. Berber, M. Lin, R. A. McCord, K. C. Ongaigui, L. D. Boxer, H. Y. Chang, K. F. Chua, Cell 2009, 136, 62–74.
- [10] E. Michishita, R. A. McCord, L. D. Boxer, M. F. Barber, T. Hong, O. Gozani, K. F. Chua, *Cell Cycle* **2009**, *8*, 2664–2666.
- [11] J. L. Feldman, J. Baeza, J. M. Denu, J. Biol. Chem. 2013, 288, 31350–31356.
- [12] M. Van Meter, Z. Mao, V. Gorbunova, A. Seluanov, Aging 2011, 3, 829–835.
- [13] R. I. Tennen, D. J. Bua, W. E. Wright, K. F. Chua, Nat. Commun. 2011, 2, 433.
- [14] A. A. Sauve, V. L. Schramm, *Biochemistry* **2003**, *42*, 9249–9256.
- [15] Y. Zhang, D. Mitchison, Int. J. Tuberc, Lung Dis. 2003, 7, 6-21.
- [16] J. Grosset, C. Truffot-Pernot, C. Lacroix, B. Ji, Antimicrob. Agents Chemother. 1992, 36, 548 – 551.
- [17] C. Manca, M. S. Koo, B. Peixoto, D. Fallows, G. Kaplan, S. Subbian, *PLoS One* 2013, 8, e74082.
- [18] C.C. Company, 2010.
- [19] M. Mayer, B. Meyer, J. Am. Chem. Soc. 2001, 123, 6108-6117.
- [20] B. Meyer, T. Peters, Angew. Chem. Int. Ed. 2003, 42, 864–890; Angew. Chem. 2003, 115, 890–918.
- [21] J. L. Avalos, K. M. Bever, C. Wolberger, *Mol. Cell* **2005**, *17*, 855–868.
- [22] P. W. Pan, J. L. Feldman, M. K. Devries, A. Dong, A. M. Edwards, J. M. Denu, J. Biol. Chem. 2011, 286, 14575 14587.
- [23] M. G. Szczepina, R. B. Zheng, G. C. Completo, T. L. Lowary, B. M. Pinto, ChemBioChem 2009, 10, 2052 – 2059.
- [24] M. Mayer, B. Meyer, Angew. Chem. Int. Ed. 1999, 38, 1784–1788; Angew. Chem. 1999, 111, 1902–1906.
- [25] H. Jiang, S. Khan, Y. Wang, G. Charron, B. He, C. Sebastian, J. Du, R. Kim, E. Ge, R. Mostoslavsky, H. C. Hang, Q. Hao, H. Lin, *Nature* **2013**, *496*, 110–113.
- [26] H. Wu, C. Tian, X. Song, C. Liu, D. Yang, Z. Jiang, Green Chem. 2013, 15, 1773 – 1789.
- [27] H. J. Koch, R. S. Stuart, Carbohydr. Res. 1978, 67, 341 348.
- [28] T. L. Hwang, A. J. Shaka, J. Magn. Reson. Ser. A 1995, 112, 275 279.

Manuscript received: December 7, 2016 Accepted Article published: February 21, 2017 Final Article published: April 18, 2017